



HAL
open science

Development of a sub-hour on-line comprehensive cation exchange chromatography x RPLC method hyphenated to HRMS for the characterization of lysine-linked antibody-drug conjugates

Soraya Chapel, Florent Rouvière, Pierre Guibal, Delphine Mathieu, Sabine Heinisch

► To cite this version:

Soraya Chapel, Florent Rouvière, Pierre Guibal, Delphine Mathieu, Sabine Heinisch. Development of a sub-hour on-line comprehensive cation exchange chromatography x RPLC method hyphenated to HRMS for the characterization of lysine-linked antibody-drug conjugates. *Talanta*, 2022, 240, pp.123174. 10.1016/j.talanta.2021.123174 . hal-03615542

HAL Id: hal-03615542

<https://hal.science/hal-03615542>

Submitted on 22 Jul 2024

HAL is a multi-disciplinary open access archive for the deposit and dissemination of scientific research documents, whether they are published or not. The documents may come from teaching and research institutions in France or abroad, or from public or private research centers.

L'archive ouverte pluridisciplinaire **HAL**, est destinée au dépôt et à la diffusion de documents scientifiques de niveau recherche, publiés ou non, émanant des établissements d'enseignement et de recherche français ou étrangers, des laboratoires publics ou privés.



Distributed under a Creative Commons Attribution - NonCommercial 4.0 International License

1 **Development of a sub-hour on-line comprehensive cation exchange**
2 **chromatography x RPLC method hyphenated to HRMS for the characterization of**
3 **lysine-linked antibody-drug conjugates**

4
5
6
7 Soraya CHAPEL^a, Florent Rouvière^a, Pierre Guibal^b, Delphine Mathieu^b, Sabine Heinisch^{a*}

8
9 ^a*Université de Lyon, Institut des Sciences Analytiques, UMR 5280, CNRS, 5 rue de la Doua, 69100,*
10 *Villeurbanne, France*

11 ^b*Sanofi Aventis R&D, 1 impasse des Ateliers, 94400 Vitry-sur-Seine, France*

12
13 ^(*)Corresponding author: Tel: +33 437 423 551, E-mail: sabine.heinisch@univ-lyon1.fr
14
15
16
17
18
19
20
21
22
23
24
25
26
27
28
29
30
31

32 **Keywords:** 2D-LC, CEX x RPLC-HRMS, lysine-linked ADC, isoforms, charge variants

33

34 **Abstract**

35 This study details the development of on-line 2D-LC methods combining cation-exchange
36 chromatography (CEX) and reversed-phase liquid chromatography (RPLC) for the separation of the
37 charge variants of a lysine-linked antibody-drug conjugate (ADC). This combination gives an excellent
38 example of the potential benefits of 2D-LC approaches for the analysis of such complex protein
39 formats. CEX is considered the reference technique for the separation of protein charge variants but
40 its retention mechanism usually requires the use of a high concentration of non-volatile salts, which
41 impedes its compatibility with MS detection. In this context, the use of an on-line 2D-LC-MS
42 approach not only allows on-line desalting and indirect coupling of CEX with MS detection but it also
43 provides increased and complementary information within a single analysis. The first part of this
44 study was devoted to the choice of stationary phases and the optimization of chromatographic
45 conditions in both dimensions. Based on the results obtained in 1D-CEX with ultraviolet detection
46 (UV) and 1D-RPLC with UV and high-resolution mass spectrometry (HRMS) detections, an on-line
47 comprehensive two-dimensional liquid chromatography method combining CEX and RPLC was
48 developed. The last part of this study was devoted to the identification of the separated species
49 using HRMS detection and in the comparison of three ADC samples exposed to different durations of
50 thermal stress.

51

52

53 1. Introduction

54 Antibody-drug conjugates (ADCs) belong to a new and fast-growing class of highly potent
55 biotherapeutic drugs targeted for the treatment of cancer, autoimmune, and inflammatory diseases
56 [1]. Structurally speaking, an ADC is composed of a monoclonal antibody (mAb) covalently linked to
57 small molecule drugs via a chemical linker. Monoclonal antibodies are highly complex “Y-shaped”
58 tetrameric glycoproteins with molecular weights near 150 kDa that are composed of two identical
59 heavy chains and two identical light chains held together by disulfide bonds [2,3]. They are thus large
60 and structurally complex molecules.

61 Product heterogeneity, introduced during manufacturing or storage, is very common for these
62 compounds but can influence biological activity, product stability, and product safety [4,5]. For this
63 reason, a comprehensive characterization of ADCs throughout their research and development
64 process is mandatory. The analytical characterization of ADCs requires the investigation and
65 monitoring of numerous critical quality attributes (CQAs), including drug distribution, average drug-
66 to-antibody ratio, amount of unconjugated mAb, site occupancy, glycosylation patterns, protein
67 aggregation, size variants, and charge variants [6]. In practice, such a thorough characterization often
68 involves multiple complementary methods based on electrophoresis, liquid chromatography (LC),
69 and mass spectrometry (MS) [6–11].

70 Over the past few years, two-dimensional liquid chromatography coupled with mass spectrometry
71 detection (2D-LC-MS) has emerged as an attractive analytical approach to address the challenges
72 associated with the characterization of these complex molecules [12–14]. They have been proven to
73 be rapid and efficient analytical tools: (i) to provide a very high resolving power by increasing the
74 overall peak capacity compared to conventional one-dimensional liquid chromatography (1D-LC) and
75 (ii) to allow MS coupling with chromatographic techniques that are not compatible with MS
76 detection to facilitate structural elucidation. The characterization of ADCs can be achieved from
77 three different and complementary approaches: top-down (analysis of intact protein), middle-up
78 (analysis after protein cleavage into large subunits between 25 and 100 kDa) or bottom-up (analysis
79 after protein cleavage into peptides < 7 kDa), each of them giving specific information on the protein.
80 Because of their potential influence on biological activity and product stability, charge variants are
81 considered as critical quality attributes of ADCs. Cation-exchange chromatography (CEX) is the gold-
82 standard technique to separate protein charge variants in liquid chromatography but it usually
83 requires a large amount of salt which makes it incompatible with MS detection. In CEX, the use of
84 volatile buffers such as ammonium acetate was reported for mAb analysis [15–19]. The main
85 problem is the salt concentration able to combine good chromatographic resolution and high MS
86 sensitivity. CEX was also successfully combined with reversed-phase liquid chromatography (RPLC) as

87 second dimension in order to (i) desalt prior to MS and (ii) provide additional selectivity for in-depth
88 characterization of mAbs and related biomolecules [20–23]. Such a combination not only allows the
89 direct assignment of ¹D-CEX peaks by MS detection but it also greatly extends, in a single analysis, the
90 level of information about the compounds present in the sample. Both the multiple heart-cutting
91 mode (mCEX-RPLC) and the selective comprehensive mode (sCEX x RPLC) were applied to mAbs
92 and/or ADCs using top-down and middle-up approaches [20,21,24]. The comprehensive mode (CEX x
93 RPLC) was also applied to mAbs using top-down and middle-up approaches [22,24,25], and to both
94 mAbs and ADCs using a bottom-up approach (i.e. analysis at the peptide level) [20,23]. Until now, on-
95 line CEX x RPLC has never been applied to the characterization of ADCs in a top-down or a middle-up
96 approach.

97 The objective of the current work was to develop an on-line comprehensive CEX x RPLC method,
98 operating in less than one hour, for in-depth characterization of the charge variants of a lysine-linked
99 antibody-drug conjugate belonging to the immunoglobulin G1 (IgG1) subclass. Herein, the focus was
100 put on the analysis of the protein samples after cleavage into large subunits following limited
101 proteolysis. In this work, the investigated ADC will be referred to as ADC-S01.

102

103 **2. Experimental section**

104 **2.1. Chemical and reagents**

105 Acetonitrile (ACN, LC-MS grade) was obtained from Sigma-Aldrich (Steinheim, Germany). Water was
106 purified and deionized by an Elga Purelab Classic UV purification system (Veolia water STI, Le Plessis
107 Robinson, France). Formic acid (FA, LC/MS grade), trifluoroacetic acid (TFA, LC/MS grade), sodium
108 chloride (NaCl), 2-(N-morpholino) ethanesulfonic acid (MES), sodium hydroxide (NaOH),
109 monosodium phosphate (NaH₂PO₄), and disodium phosphate (Na₂HPO₄), all analytical grade, were
110 obtained from Fischer scientific (Illkirch, France). IdeS protease enzyme (FabRICATOR) was obtained
111 from Genovis (Lund, Sweden).

112 The investigated samples of ADC-S01 were provided by Sanofi Aventis R&D (Vitry sur Seine, France)
113 and were formulated at 5 mg/mL. Thermally-stressed samples were obtained by exposing ADC-S01
114 to elevated temperature (40°C) for either two weeks or four weeks. In this work, the unstressed,
115 stressed for two weeks, and stressed for four weeks samples will be referred to as ADC-t0, ADC-t2,
116 and ADC-t4, respectively.

117

118 **2.2. Sample preparation**

119

120 The antibody-drug conjugate studied was a lysine-linked ADC incorporating an antibody of the
121 immunoglobulin G1 (IgG1) isotype with isoelectric points ranging from 8.5 for the naked mAb to 7.1
122 for most conjugated species. ADC samples were injected at their formulated concentration, without
123 any pre-treatment nor prior dilution. Partially digested ADC samples were obtained using IdeS
124 protease enzyme (FabRICATOR) following the instructions provided by the manufacturer (i.e. one
125 unit of enzyme/ μg of ADC incubated at 37°C for 30 min). Partial digestion with IdeS cleaves the
126 protein below the hinge region of the heavy chain, which leads to the formation of two Fc/2 subunits
127 and one F(ab')₂ subunit [26].

128

129 **2.3. Columns**

130 Two columns were evaluated for the first CEX dimension: BioResolve SCX (100 x 2.1 mm, 3 μm) from
131 Waters (Milford, MA, USA) and Bio MAb NP5 (250 x 2.1 mm, 5 μm) from Agilent Technologies
132 (Waldbronn, Germany).

133 Five columns were evaluated for the second RPLC dimension: BioResolve RP mAb polyphenyl (50 x
134 2.1 mm, 2.7 μm) and Acquity BEH C4 (50 x 2.1 mm, 1.7 μm) from Waters (Milford, MA, USA), Biozen
135 intact XB-C8 (50 x 2.1, 3.6 μm) from Phenomenex (Torrence, CA, USA), PLRP-S (50 x 2.1mm, 5 μm)
136 and AdvanceBio RP-mAb diphenyl (50 x 2.1mm, 3.5 μm) from Agilent Technologies (Waldbronn,
137 Germany).

138

139 **2.4. Instrumentation**

140 1D-LC-UV column evaluations were carried out with an Acquity UPLC liquid chromatography system
141 from Waters (Milford, MA, USA). The instrument includes a high-pressure binary solvent delivery
142 pump, a sample manager with a 20- μL loop, a column manager equipped with a column oven with a
143 maximum temperature of 90°C, and a diode-array detector equipped with a 0.5- μL flow-cell
144 withstanding pressure up to 70 bar. The dwell volume and extra-column volume for this entire
145 system were measured using a zero-dead volume union connector in place of the column and were
146 respectively 110 μL and 12 μL .

147 Other 1D-LC-UV-HRMS experiments were carried out using the first dimension of a 1290 Infinity
148 series 2D-LC system (see description of the instrument below).

149 On-line LC x LC experiments were carried out using a 1290 Infinity series 2D-LC system from Agilent
150 Technologies (Waldbronn, Germany). The instrument includes two high-pressure binary solvent
151 delivery pumps, an autosampler with a flow-through needle of 20 μL equipped with a 160- μL

152 extension loop when needed, two thermostated column compartments with a maximum
153 temperature of 100 °C equipped with low-dispersion preheaters, and two diode-array detectors
154 equipped with 0.6- μ L flow-cells.

155 The interface connecting the two dimensions consisted of a 2-position/4-port duo valve, equipped
156 with two identical 80- μ L loops. To minimize dispersion, the valve was configured in back-flush
157 injection mode. A pressure release kit placed between the ¹D-outlet and the interface was used to
158 minimize the pressure downstream induced by the switch of the 2D-LC valve to protect the flow-cell
159 and avoid artefacts in the signal. The measured dwell volumes and extra-column volumes of this 2D-
160 LC system were respectively 170 μ L and 22 μ L in ¹D, and 80 μ L and 8.5 μ L in ²D (loop volume at the
161 interface excluded).

162 The 2D-LC system was hyphenated to an Agilent G6560B Q-TOF mass spectrometer, equipped with a
163 JetStream electrospray ionization (ESI) source. For the LC x LC experiment, a diverter valve was
164 placed between the 2D-LC and MS instruments to redirect part of the ²D-effluent to the waste
165 following each injection and prevent contamination of the MS source with non-volatile NaCl.

166 Data acquisition and instrument control were performed using Agilent OpenLab software for 2D-LC
167 and MassHunter software for MS.

168 MS data processing was performed using Agilent MassHunter qualitative analysis software for MS
169 data and Agilent BioConfirm software for deconvolution of the MS spectra. 2D-LC data were
170 processed using an in-house script developed on Matlab.

171

172 **2.5. Chromatographic and detection conditions**

173 The analytical conditions used in 1D-CEX and 1D-RPLC for developing and optimizing the 2D-LC
174 methods are specified in the respective figure captions and in the text.

175 The conditions for the optimized CEX x RPLC method are given in Table 1.

176

177 **3. Results and discussion**

178 **3.1. Development and optimization of 2D-LC conditions**

179 A 2D-LC separation is the combination of two 1D-LC experiments. As part of method development,
180 each dimension (i.e. CEX on one hand and RPLC on the other hand) was individually optimized with a
181 view to maximize the separation power. The investigated parameters were: the nature of the

182 stationary phase, the nature and the composition of the mobile phase, the gradient conditions, and
183 the injection conditions.

184

185 **3.1.1. Choice of stationary phase and mobile phase buffer in 1D-CEX**

186 The first step of this study aimed at finding a suitable CEX method for separating charge variants in
187 the first dimension. For this purpose, we evaluated several stationary phases and mobile phase
188 buffers. In the literature, the Agilent Bio MAb NP5 column was exclusively used in ¹D-CEX for the 2D-
189 LC separation of mAbs and related products [20–22], with either MES [20,21], phosphate [20] or
190 ammonium acetate [22] as mobile phase buffers.

191 In addition to this column, we evaluated the BioResolve SCX column from Waters. Both columns are
192 packed with non-porous polymeric-based particles and are specifically designed for the separation of
193 the charge isoforms of biotherapeutic proteins. Non-porous polymeric particles are usually preferred
194 for protein analysis in CEX. They enable to work across a wide range of mobile phase pH and provide
195 better chromatographic performance by limiting trans-particle mass transfer resistance [27], which
196 can be a critical issue for large proteins. The Bio MAb NP5 column contains weak cation-exchange
197 sites (WCX), whereas the BioResolve SCX column contains strong cation-exchange ones (SCX).
198 Because SCX phases employ strong acids, the number of charges on their surface is expected to
199 remain constant over a broad pH range, which makes them attractive in CEX. In contrast, WCX
200 phases employ weak acids that gradually lose their ionization when the pH decreases below pH 5
201 [28]. It is important to be aware of such limitations during method development. However, it should
202 be pointed out that, in our study, the conditions were operated over a small pH range between 6.5
203 and 7.6, in which both columns are expected to deliver optimal performance.

204 In CEX, protein elution may be performed with either salt gradients, pH gradients or salt-mediated
205 pH gradients (combined salt/pH gradients) [28–30]. In this work, we used a classical salt gradient for
206 the separation, as this is the most frequently used mode for the separation of protein charge variants
207 [28]. Sodium chloride (NaCl) was used for the salt gradient while two different mobile phase buffers
208 were evaluated for the separation (MES and phosphate). In CEX, the separation mechanism relies on
209 the binding of positively charged analytes on a negatively charged stationary phase. Because a
210 positive charge is removed from the molecule when a lysine is conjugated with a drug, increasing
211 drug conjugation is expected to lead to decreasing retention. For this reason, the influence of the
212 mobile phase pH on the separation was also investigated. Analyte retention was found to be
213 insufficient above pH 7.6 and the best separation was achieved with pH 6.5 (Fig. S1), which was

214 expected given the isoelectric point range ($7.3 < pI < 8.5$) of the expected isoforms (8.5
215 corresponding to the non-conjugated mAb).

216 Evaluation of the two sets of stationary phase and mobile phase buffers was performed on IdeS-
217 treated ADC-S01 sample at pH 6.5. The results obtained for this comparison are shown in Fig. 1,
218 which draws attention to the effect of the buffer for a given column (Bio MAb in Fig. 1a and
219 BioResolve in Fig. 1b). As can be seen, overall, the separations were quite similar with the two
220 columns. Although the Bio Mab NP5 column gave slightly better peak separation and resolution than
221 the BioResolve SCX column, no significant differences were found between the two columns.
222 Therefore, we made a decision based on column dimensions and selected the BioResolve SCX column
223 to keep the analysis time as short as possible in 2D-LC (shorter column length allowing shorter
224 gradient time in ¹D). As shown in Fig. 1b, the MES buffer gave slightly better separation than the
225 phosphate buffer and was thus selected for the ¹D-CEX. These results are in line with the work of
226 Baek et al. [31] who reported a better separation for model proteins using MES buffer compared to
227 phosphate buffer at the same pH. Those results were attributed to the zwitterionic nature of MES.
228 This latter buffer allows for better control of pH at the surface of the column resin. It also removes
229 interactions with protein charges, unlike the phosphate buffer.

230 With a view to minimize the dilution factor in ¹D, a brief study of the effect of the injected volume on
231 the separation was conducted. No deterioration in peak shape was observed up to an injection
232 volume of 80 μ L (see Fig S2). This is mainly due to the excellent focusing at the head of the column
233 when injecting in CEX a sample diluted in water.

234

235 **3.1.2. Choice of stationary phase and mobile phase additive in 1D-RPLC**

236 For the analysis of ADCs in top-down and/or middle-up, the use of a ²D-RPLC separation after a ¹D-
237 CEX separation provides two benefits: (i) it allows the indirect on-line coupling of CEX with MS
238 detection and (ii) it potentially brings an additional and complementary separation to the ¹D-CEX.

239 Because the cytotoxic drugs are hydrophobic, the process of drug conjugation increases the
240 hydrophobicity of the molecule. A separation by increasing drug load or drug-to-antibody (DAR) can
241 thus be expected in RPLC. In this work, RPLC conditions were optimized keeping two main objectives
242 in mind: (i) maximizing peak separation and (ii) allowing sufficient mass spectrometric sensitivity for
243 peak identification.

244 In RPLC-MS analysis of proteins, the selection of the mobile phase additive is a key parameter during
245 method development. Due to its strong hydrophobic, acidic, and ion-pairing characters,

246 trifluoroacetic acid (TFA) is well-known to provide the best chromatographic results for the
247 separation of proteins in RPLC [32–34]. However, it is also well-known to provide a dramatic
248 decrease in MS detection sensitivity due to analyte ionization suppression and spray instability.
249 Decreasing the concentration of TFA in the mobile phase was demonstrated to be an effective
250 strategy to preserve the chromatographic separation while maintaining enough MS sensitivity [35].
251 In this work, the influence of the concentration of TFA in the mobile phase on the separation was
252 investigated on intact and IdeS-treated ADC-S01 samples. Fig. S3 shows 1D-RPLC-UV separations of
253 both samples using 0.1% TFA (Fig. S3a) or 0.05% TFA + 0.1% FA (Fig. S3b) in the mobile phase.
254 Decreasing the concentration of TFA in the mobile phase from 0.1% to 0.05% had no significant
255 impact on chromatographic performance while significantly increasing MS sensitivity. It was reported
256 that below 0.05%, the recovery of intact proteins decreased due to adsorption on the stationary
257 phase [36]. We therefore selected a concentration of 0.05% TFA in the mobile phase for the rest of
258 this study.

259 Several stationary phases were investigated for the second dimension. Except for the non-porous
260 polymeric-based PLRP-S column, all columns contained silica-based particles with either C4 alkyl-
261 (Acquity BEH C4), C8 alkyl- (Biozen intact XB-C8), diphenyl- (AdvanceBio RP-Mab diphenyl) or
262 polyphenyl ligands (BioResolve RP mAb Polyphenyl) bonded to superficially porous particles. Non-
263 porous and superficially porous particles are usually preferred for protein analysis in RPLC as they
264 limit mass transfer resistance [37]. Fig. 2 shows a comparison of RPLC-UV separations of intact and
265 IdeS-treated ADC-S01 samples obtained with each of these stationary phases. From a
266 chromatographic standpoint, the best results were obtained with the Bioresolve RP mAb column (Fig.
267 2a). The Agilent PLRP-S column (Fig. 2b) also showed good performance and could have been
268 attractive to prevent high temperature-related silica bleeding in ²D as it is a polymeric-based column.
269 However, the very low pressure limit of this column (< 200 bar) makes it incompatible with the high
270 flow rates that are required in ²D. The Acquity BEH C4 column was also evaluated but showed poorer
271 performance than the BioResolve RP mAb column. The comparison between these two columns can
272 be found in Fig. S4.

273

274 **3.1.3. Determination of the useful separation space in RPLC**

275 To better optimize the second RPLC dimension, IdeS-treated ADC-S01 sample was analyzed in 1D-
276 RPLC using both UV and HRMS detections. As shown in Fig. 3a (UV) and Fig. 3b (MS), the area of
277 interest in the chromatogram (i.e. the time interval during which the species of interest elute) was
278 found to be very short relative to the entire separation space. The useful separation space ranged

279 from about 2.5 min to 4.4 min with a gradient elution ranging from 20% to 95% B in 8.8 min. This
280 area of interest was delimited after identifying the separated peaks based on their exact masses
281 using HRMS detection. The peaks of interest are labelled from 1 to 7 in Fig. 3b and the corresponding
282 assignments are given in Table 2. Assignments were made by comparing experimentally the
283 measured masses with the expected theoretical masses. Species corresponding to Fc/2 subunits with
284 1 or 2 drugs were identified in the first part of the area of interest, whereas F(ab')₂ subunits with
285 drug loads from 0 to 5 were found in the second part. Several peaks with very close masses but
286 different retention times were observed (e.g. peak #3, #4, #5, and #6a), suggesting the presence of
287 isomeric compounds. The presence of distinct subunits with identical drug load in RPLC could be
288 explained by drug conjugation at different lysine residues. Similar results were reported for the
289 analysis of the commercialized lysine-conjugated ADC ado-trastuzumab emtansine (Kadcyla[®]) in
290 mCEX-RPLC [20].

291 In the two samples that were analyzed (i.e. intact ADC and IdeS-treated ADC), the presence of
292 numerous interfering peaks that could correspond to various polymer excipients was highlighted in
293 the second half of the chromatogram (label #8 in Fig. 3b). Excipients were non-ionic surfactants used
294 to prevent protein aggregation. In our study, those compounds were found to be strongly retained in
295 RPLC due to the lipophilic part which exhibits strong hydrophobicity. Most of them were more
296 retained than the species of interest. However, some of the earliest eluted excipients were found to
297 coelute with the latest eluted species of interest and appeared to create significant ion suppressions
298 in MS.

299

300 **3.2. On-line CEX x RPLC analysis of IdeS-digested ADC-S01**

301 In the context of top-down and/or middle-up analysis of mAb and ADC, both on-line multiple heart-
302 cutting mCEX-RPLC (for ADC) [20] and full comprehensive CEX x RPLC (for mAb) [21,22] were
303 reported in the literature.

304 Before fully optimizing the conditions in CEX x RPLC, we performed an on-line CEX x RPLC analysis to
305 study the retention of the excipients in CEX and determine whether or not these compounds could
306 be eliminated in ¹D. Fig. 4 shows the contour plot obtained for the analysis of the IdeS-treated ADC
307 sample using MS detection. As seen, most of the excipients eluted before the delimited area of
308 interest in ¹D-CEX (i.e. before 5 min) whereas only a small part of them (highlighted by a black circle)
309 coeluted with the species of interest. It should be pointed out that, contrary to the observations

310 made in 1D-RPLC-HRMS (Fig. 3b), the different excipients elute all along the RPLC separation making
311 MS signal intensity too low to unambiguously identify F(ab')₂ species in ²D-RPLC.

312 As previously underlined, the separation space was quite small in ¹D-CEX. All compounds eluted
313 before 12 min with a gradient elution ranging from 1% to 40% B in about 40 min. Considering the
314 reduced elution range in ¹D, the conditions in CEX was later further optimized by decreasing the
315 upper composition range to decrease the gradient slope and hence improve the separation.

316 Conditions were further optimized in full comprehensive mode, keeping three main objectives in
317 mind: (i) removing interfering excipients as much as possible, (ii) finding sub-hour conditions, and (iii)
318 maximizing MS-detection sensitivity. Given the limited elution range in CEX, the gradient time was
319 set at 20 min with gradient compositions ranging from 1% to 17% B (total analysis time = 31.3 min).
320 The sampling time and hence the analysis time in ²D was set at 0.78 min to maintain 2 to 3 fractions
321 per ¹D-peak and minimize undersampling [38]. The strategy used to avoid MS signal suppression
322 arising from coelutions with excipient species was to take advantage of their low retention in ¹D-CEX
323 and remove them as much as possible before starting to send the fractions to ²D-RPLC. As highlighted
324 in Fig. S5, to improve the chromatographic separation while keeping a short gradient time, the
325 gradient composition range was reduced from 30-95% B to 30-50% B. The resulting optimized
326 conditions for this comprehensive 2D-LC method are given in Table 1. The gradient time in CEX with
327 this column size (i.e. 10 cm) was increased as much as possible (i.e. 20 min), resulting in a total
328 analysis time of 30 min. An increase in the gradient time up to 60 min resulted in a decrease in
329 sensitivity without a significant gain in peak capacity.

330 Fig. 5 shows the resulting on-line CEX x RPLC separations of IdeS-treated ADC-S01 sample using MS
331 detection. The separated peaks are labelled from 1 to 21 and the proposed assignments for each
332 peak are given in Table 3. As aforementioned, the 2D-LC conditions were optimized in each
333 dimension to maximize the peak capacity and eliminate the excipient species that were found to
334 impact MS sensitivity. The composition range was reduced in both dimensions to fit the elution range
335 of the species of interest regardless of the excipients. These species could be removed from the
336 separation space of interest by starting to send the fractions in ²D from 4 min or 5 min depending on
337 the conditions (see Table 1).

338 As seen in Fig. 5, this comprehensive method led to a good separation of Fc/2 and F(ab')₂ species in
339 both dimensions. It is interesting to point out the good complementarity of the two chromatographic
340 techniques for the separation of these species. Multiple peaks are observed on the contour plot,
341 some of which being well separated in CEX but not in RPLC, and vice-versa. For example, peaks #7
342 and #15 have very similar retention times in ¹D which means that these two compounds would have

343 coeluted in a single 1D-CEX separation. The two peaks are, on the other hand, easily separated in ²D.
344 Similarly, peaks #7 and #8 mainly coelute in ²D but are well separated in ¹D. This underlines that
345 different and complementary selectivities are provided by the two dimensions.

346 Several peaks are observed on the contour plot, which indicates a large number of isoforms in the
347 analyzed sample. Distinct species with the same measured mass that were identified as Fc/2 subunits
348 with one drug were found to be separated in one or both dimensions (e.g. peaks #1 to #8). In
349 addition, F(ab')₂ fragments with drug loads from 1 to 3 could be identified in the second part of the
350 contour plot. Similarly to the Fc/2 species, a few isobars identified as F(ab')₂ with the same number
351 of drugs were separated in CEX x RPLC (e.g. peaks #13 and #18 or peaks #16, #19 and #20). As
352 pointed out before, some of these species could correspond to subunits with the same number of
353 drugs but conjugated at different lysine residues. Differences in conjugated sites could explain
354 differences in retention in RPLC for subunits displaying the same drug load (e.g. peaks #3, #5, and
355 #7). However, such an explanation does not work for species separated in ¹D-CEX since such
356 differences should not impact the net charge of the molecule (e.g. peaks #7, #8, and #9). For those
357 compounds, the different peaks exhibiting the same mass that we observe could be the result of
358 post-translational modifications (PTMs) that would change the charge and/or hydrophobicity of the
359 molecule while creating very small mass differences (barely detectable in MS), such as deamidation,
360 isomerization or racemization among others [10,22].

361 To summarize, as indicated in Table 3, Fc/2 subunits with 1 and 2 drugs, as well as F(ab')₂ subunits
362 with 0, 1, 2, and 3 drugs could be unambiguously identified using HRMS detection. Unlike in 1D-RPLC,
363 F(ab')₂ subunits with 4 and 5 drugs could not be identified in CEX x RPLC due to the limited MS signal
364 obtained for these large fragments. Based on its retention times in both dimensions (peak least
365 retained in CEX but most retained in RPLC), we suspected peak #21 to be a F(ab)₂ fragment with a
366 drug load of 4. However, the signal was too low for proper MS spectrum deconvolution. Considering
367 the retention time of peak #21, it is most likely that any F(ab')₂ fragments with a drug load of 5
368 eluted before the first analyzed ¹D-fraction (i.e. before 5 min), which explains their absence in the
369 chromatogram. It should be pointed out that some very large mass differences were sometimes
370 observed between experimental and expected theoretical masses (cf. Tables 2 and 3). Those
371 differences can be attributed to post-translational modifications, especially oxidation or linker and
372 drug modification due to thermal stress.

373 To improve MS sensitivity, we tried to increase the injected volume in ¹D-CEX (from 40 μL to 80 μL).
374 As expected, increasing the injected volume from 40 μL (Fig. S6a) to 80 μL (Fig. S6c) resulted in a 2-
375 fold increase in peak intensity in UV in the second dimension without affecting the separation.

376 However, as seen in Figs. S6b vs. S6d, poorer results were obtained in MS detection due to a
377 significant increase of background noise that counteracted the expected increase of signal-to-noise
378 (S/N) ratio. Consequently, increasing the injected volume in ¹D-CEX did not facilitate MS
379 identification in ²D-RPLC as expected but rather made it more difficult. This increase in background
380 noise in ²D when doubling the injected volume in ¹D is probably the result of increased matrix effects.

381 Fig. 5 also highlights the species that were identified in the IdeS-digested ADC-S01 sample in on-line
382 CEX x RPLC. As can be expected, ²D-RPLC allowed separating Fc/2 species from F(ab')₂ species on one
383 hand, and Fc/2 subunits according to their drug load on the other hand. F(ab')₂ subunits with
384 different drug load were poorly separated in RPLC while well separated in ¹D-CEX. As can be
385 expected, the most retained F(ab')₂ fragment in CEX was the one with the lowest drug load (0 in this
386 case). Conversely, RPLC was very useful to discriminate F(ab')₂ fragments exhibiting a close mass,
387 whereas Fc/2 fragments exhibiting a close mass were better separated in CEX. Each black rectangle in
388 Fig. 5 includes one or several peaks identified as F(ab')₂ fragments with the same drug load.
389 Interestingly, the most retained isoform in CEX was also the most retained one in RPLC, although the
390 shift in retention was very subtle in CEX. This suggests that those additional variants might be the
391 result of post-translational modifications (PTMs) that would simultaneously increase the net negative
392 charge and the hydrophobicity of the protein.

393

394 **3.3. Application of developed method to stability study**

395 The stability of biotherapeutic antibodies is a critical quality attribute that is essential to assess to
396 support formulation development, understand degradation pathways, and evaluate product shelf
397 life, among other objectives [39]. The applicability of the developed on-line CEX x RPLC-UV-HRMS
398 method to stability studies was investigated by analyzing three different IdeS-treated ADC samples: a
399 non-stressed sample (ADC-t₀), a sample stressed at 40°C for two weeks (ADC-t₂), and a sample
400 stressed at 40°C for four weeks (ADC-t₄).

401 Fig. 6 shows the contour plots obtained in UV detection for the three samples. First of all, the 2D
402 method was found to be highly repeatable between analyses (in terms of retention times), which
403 allowed easy and fast comparison of the 2D maps. As mentioned before, the two dimensions were
404 very complementary for the separation of these species. The direct visual comparison of the 2D maps
405 showed marked differences between the three IdeS-digested samples. The most striking differences
406 are indicated by black dotted circles (see Table 3 for corresponding identifications). For the large
407 majority of peaks, intensities decrease from t₀-IdeS to t₄-IdeS (i.e. #1-6, 9, 10, 11, 13, and 17), until
408 even completely disappearing for some peaks (e.g. #9, 10, and 11). These peaks correspond to Fc/2

409 with 1 drug (#1-6 and 9), Fc/2 with 2 drugs (#10 and 11), F(ab')₂ with 1 drug (#18 and 19), and F(ab')₂
410 with 2 drugs (#13 and 17). Other peaks, initially absent in t0-IdeS, progressively appear in the
411 chromatogram (i.e. #22, which could not be identified). Lastly, for other species (i.e. # 16, 18, 19, and
412 21), the peak intensity increases from t0-IdeS to t2-IdeS but decreases from t2-IdeS to t4-IdeS. Those
413 results emphasize the great potential of using on-line LC x LC for stability studies during ADC research
414 and development.

415

416 **4. Conclusion and future prospects**

417 This work has led to the development of on-line CEX x RPLC-UV-HRMS method for an extensive
418 characterization of the charge variants of a lysine-linked antibody-drug conjugate in less than 30 min.

419 The good complementarity between the two combined dimensions (CEX and RPLC) provided much
420 insight into the different isoforms present in this sample and highlighted the existence of numerous
421 species with very similar masses, possibly resulting from drug conjugations on different lysine
422 residues or post-translational modifications. Fc/2 sub-units with 1 and 2 drugs on one hand, and
423 F(ab')₂ sub-units with drug loads from 0 to 5 drugs could be identified in the IdeS-digested sample.
424 Direct comparison of 2D maps obtained from samples subjected to temperature-induced stress
425 provided valuable information on possible modifications resulting from sample degradation.

426 One of the major issue encountered in this work was the limited MS detection sensitivity, which
427 impeded deconvolution of some MS spectra, and thus peak identification. This limited sensitivity was
428 ascribed to (i) the formation of highly multi-charged ions reducing peak intensity, (ii) the presence of
429 TFA in the mobile phase, creating ion suppression, (iii) the omnipresence of excipients also creating
430 ion suppression, and (iv) the high-salt content coming from ¹D-CEX, which might impact ionization
431 efficiency despite the use of a diverted valve before MS (as suggested by the large amount of white
432 deposits observed on the source cone at the end of each analysis). Possible solutions to alleviate the
433 latter issue could consist in using more volatile buffers as the buffer combinations reported for the
434 analysis of mAbs in 1D-CEX-MS [15–19] or in on-line CEX x RPLC-MS [22].

435 Besides an extensive optimization of the ESI-MS ionization conditions, other options to improve MS
436 sensitivity could involve (i) a further reduction of the flow entering MS employing larger flow splitting
437 ratios [40], (ii) the introduction of a make-up flow prior to MS in order to decrease TFA concentration
438 without impacting the chromatographic separation [40,41] or (iii) the use of alternative mobile phase
439 additives as was recently done for mAbs [42]. The three options were discussed by d'Atri et al. [37] in
440 a recent review, focusing on current trends in RPLC analysis of therapeutic proteins.

441 To further improve both separation and detection sensitivity, the potential of other chromatographic
442 combinations such as HILIC and RPLC could be investigated. The interest of this combination was
443 previously demonstrated for the separation of partially digested mAbs [25] and peptides [23,43].
444 HILIC requires less MS-incompatible salts for the separation compared to CEX, which could be
445 attractive for reducing ion suppression. However, this combination is also known to be very
446 challenging for the separation of peptides and proteins due to injection issues arising from solvent
447 strength mismatch in both dimensions [23,25,43]. Finally, the separation power should be improved
448 by increasing the gradient time in ¹D but at the cost of longer analysis times and larger sample
449 amounts to maintain similar sensitivity.

450

451 **Acknowledgements**

452 The authors thank Eric Nebel (Agilent Technologies) for the gift of columns.

453 This work was funded by Sanofi Aventis, the University of Lyon and the Centre National de la
454 Recherche Scientifique (CNRS).

455

456

457 **References**

- 458 [1] R.-M. Lu, Y.-C. Hwang, I.-J. Liu, C.-C. Lee, H.-Z. Tsai, H.-J. Li, H.-C. Wu, Development of
459 therapeutic antibodies for the treatment of diseases, *J. Biomed. Sci.* 27 (2020) 1.
460 <https://doi.org/10.1186/s12929-019-0592-z>.
- 461 [2] A. Beck, L. Goetsch, C. Dumontet, N. Corvaia, Strategies and challenges for the next generation
462 of antibody-drug conjugates, *Nat. Rev. Drug. Discov.* 16 (2017) 315–337.
463 <https://doi.org/10.1038/nrd.2016.268>.
- 464 [3] A. Beck, T. Wurch, C. Bailly, N. Corvaia, Strategies and challenges for the next generation of
465 therapeutic antibodies, *Nat. Rev. Immunol.* 10 (2010) 345–352.
466 <https://doi.org/10.1038/nri2747>.
- 467 [4] S. Panowski, S. Bhakta, H. Raab, P. Polakis, J.R. Junutula, Site-specific antibody drug conjugates
468 for cancer therapy, *MAbs* 6 (2013) 34–45. <https://doi.org/10.4161/mabs.27022>.
- 469 [5] P.L. Ross, J.L. Wolfe, Physical and chemical stability of antibody drug conjugates: Current status,
470 *J. Pharm. Sci.* 105 (2016) 391–397. <https://doi.org/10.1016/j.xphs.2015.11.037>.
- 471 [6] A. Wagh, H. Song, M. Zeng, L. Tao, T.K. Das, Challenges and new frontiers in analytical
472 characterization of antibody-drug conjugates, *MAbs* 10 (2018) 222–243.
473 <https://doi.org/10.1080/19420862.2017.1412025>.
- 474 [7] S. Fekete, A.-L. Gassner, S. Rudaz, J. Schappler, D. Guillarme, Analytical strategies for the
475 characterization of therapeutic monoclonal antibodies, *TrAC - Trends Anal. Chem.* 42 (2013)
476 74–83. <https://doi.org/10.1016/j.trac.2012.09.012>.
- 477 [8] S. Fekete, D. Guillarme, P. Sandra, K. Sandra, Chromatographic, Electrophoretic, and mass
478 spectrometric methods for the analytical characterization of protein biopharmaceuticals, *Anal.*
479 *Chem.* 88 (2016) 480–507. <https://doi.org/10.1021/acs.analchem.5b04561>.
- 480 [9] B. Bobály, S. Fleury-Souverain, A. Beck, J.-L. Veuthey, D. Guillarme, S. Fekete, Current
481 possibilities of liquid chromatography for the characterization of antibody-drug conjugates, *J.*
482 *Pharm. Biomed. Anal.* 147 (2018) 493–505. <https://doi.org/10.1016/j.jpba.2017.06.022>.
- 483 [10] A. Beck, E. Wagner-Rousset, D. Ayoub, A. Van Dorsselaer, S. Sanglier-Cianféroni,
484 Characterization of therapeutic antibodies and related products, *Anal. Chem.* 85 (2013) 715–
485 736. <https://doi.org/10.1021/ac3032355>.
- 486 [11] A. Beck, V. D’Atri, A. Ehkirch, S. Fekete, O. Hernandez-Alba, R. Gahoual, E. Leize-Wagner, Y.
487 Francois, D. Guillarme, S. Cianféroni, Cutting-edge multi-level analytical and structural
488 characterization of antibody-drug conjugates: present and future, *Expert Rev. Proteom.* 16
489 (2019) 337–362. <https://doi.org/10.1080/14789450.2019.1578215>.
- 490 [12] J. Camperi, A. Goyon, D. Guillarme, K. Zhang, C. Stella, Multi-dimensional LC-MS: the next
491 generation characterization of antibody-based therapeutics by unified online bottom-up,
492 middle-up and intact approaches, *Analyst* 146 (2021) 747–769.
493 <https://doi.org/10.1039/D0AN01963A>.
- 494 [13] B.W.J. Pirok, D.R. Stoll, P.J. Schoenmakers, Recent developments in two-dimensional liquid
495 chromatography: Fundamental improvements for practical applications, *Anal. Chem.* 91 (2019)
496 240–263. <https://doi.org/10.1021/acs.analchem.8b04841>.
- 497 [14] D. Stoll, J. Danforth, K. Zhang, A. Beck, Characterization of therapeutic antibodies and related
498 products by two-dimensional liquid chromatography coupled with UV absorbance and mass
499 spectrometric detection, *J. Chromatogr. B* 1032 (2016) 51–60.
500 <https://doi.org/10.1016/j.jchromb.2016.05.029>.
- 501 [15] Y. Leblanc, C. Ramon, N. Bihoreau, G. Chevreux, Charge variants characterization of a
502 monoclonal antibody by ion exchange chromatography coupled on-line to native mass
503 spectrometry: Case study after a long-term storage at +5°C, *J. Chromatogr. B* 1048 (2017) 130–
504 139. <https://doi.org/10.1016/j.jchromb.2017.02.017>.

- 505 [16] A.O. Bailey, G. Han, W. Phung, P. Gazis, J. Sutton, J.L. Josephs, W. Sandoval, Charge variant
506 native mass spectrometry benefits mass precision and dynamic range of monoclonal antibody
507 intact mass analysis, *MABs* 10 (2018) 1214–1225.
508 <https://doi.org/10.1080/19420862.2018.1521131>.
- 509 [17] Y. Yan, A.P. Liu, S. Wang, T.J. Daly, N. Li, Ultrasensitive characterization of charge heterogeneity
510 of therapeutic monoclonal antibodies using strong cation exchange chromatography coupled to
511 native mass spectrometry, *Anal. Chem.* 90 (2018) 13013–13020.
512 <https://doi.org/10.1021/acs.analchem.8b03773>.
- 513 [18] F. Füssl, A. Trappe, K. Cook, K. Scheffler, O. Fitzgerald, J. Bones, Comprehensive characterisation
514 of the heterogeneity of adalimumab via charge variant analysis hyphenated on-line to native
515 high resolution Orbitrap mass spectrometry, *MABs* 11 (2018) 116–128.
516 <https://doi.org/10.1080/19420862.2018.1531664>.
- 517 [19] F. Füssl, K. Cook, K. Scheffler, A. Farrell, S. Mittermayr, J. Bones, Charge variant analysis of
518 monoclonal antibodies using direct coupled pH gradient cation exchange chromatography to
519 high-resolution native mass spectrometry, *Anal. Chem.* 90 (2018) 4669–4676.
520 <https://doi.org/10.1021/acs.analchem.7b05241>.
- 521 [20] K. Sandra, G. Vanhoenacker, I. Vandenheede, M. Steenbeke, M. Joseph, P. Sandra, Multiple
522 heart-cutting and comprehensive two-dimensional liquid chromatography hyphenated to mass
523 spectrometry for the characterization of the antibody-drug conjugate ado-trastuzumab
524 emtansine, *J. Chromatogr. B* 1032 (2016) 119–130.
525 <https://doi.org/10.1016/j.jchromb.2016.04.040>.
- 526 [21] D.R. Stoll, D.C. Harmes, J. Danforth, E. Wagner, D. Guillaume, S. Fekete, A. Beck, Direct
527 identification of rituximab main isoforms and subunit analysis by online selective
528 comprehensive two-dimensional liquid chromatography–mass spectrometry, *Anal. Chem.* 87
529 (2015) 8307–8315. <https://doi.org/10.1021/acs.analchem.5b01578>.
- 530 [22] M. Sorensen, D.C. Harmes, D.R. Stoll, G.O. Staples, S. Fekete, D. Guillaume, A. Beck, Comparison
531 of originator and biosimilar therapeutic monoclonal antibodies using comprehensive two-
532 dimensional liquid chromatography coupled with time-of-flight mass spectrometry, *MABs* 8
533 (2016) 1224–1234. <https://doi.org/10.1080/19420862.2016.1203497>.
- 534 [23] G. Vanhoenacker, I. Vandenheede, F. David, P. Sandra, K. Sandra, Comprehensive two-
535 dimensional liquid chromatography of therapeutic monoclonal antibody digests, *Anal. Bioanal.*
536 *Chem.* 407 (2015) 355–366. <https://doi.org/10.1007/s00216-014-8299-1>.
- 537 [24] S. Jaag, M. Shirokikh, M. Lämmerhofer, Charge variant analysis of protein-based
538 biopharmaceuticals using two-dimensional liquid chromatography hyphenated to mass
539 spectrometry, *J. Chromatogr. A* 1636 (2021) 461786.
540 <https://doi.org/10.1016/j.chroma.2020.461786>.
- 541 [25] D.R. Stoll, D.C. Harmes, G.O. Staples, O.G. Potter, C.T. Dammann, D. Guillaume, A. Beck,
542 Development of comprehensive online two-dimensional liquid chromatography/mass
543 spectrometry using hydrophilic interaction and reversed-phase separations for rapid and deep
544 profiling of therapeutic antibodies, *Anal. Chem.* 90 (2018) 5923–5929.
545 <https://doi.org/10.1021/acs.analchem.8b00776>.
- 546 [26] Genovis » FabRICATOR. <https://www.genovis.com/products/igg-proteases/fabricator/>
547 (accessed September 27, 2021).
- 548 [27] S. Fekete, A. Beck, J.-L. Veuthey, D. Guillaume, Ion-exchange chromatography for the
549 characterization of biopharmaceuticals, *Journal of Pharmaceutical and Biomedical Analysis* 113
550 (2015) 43–55. <https://doi.org/10.1016/j.jpba.2015.02.037>.
- 551 [28] E. Farsang, D. Guillaume, J.-L. Veuthey, A. Beck, M. Lauber, A. Schmuldach, S. Fekete, Coupling
552 non-denaturing chromatography to mass spectrometry for the characterization of monoclonal
553 antibodies and related products, *Journal of Pharmaceutical and Biomedical Analysis* 185 (2020)
554 113207. <https://doi.org/10.1016/j.jpba.2020.113207>.

- 555 [29] E. Farsang, A. Murisier, K. Horváth, A. Beck, R. Kormány, D. Guillarme, S. Fekete, Tuning
556 selectivity in cation-exchange chromatography applied for monoclonal antibody separations,
557 part 1: Alternative mobile phases and fine tuning of the separation, *Journal of Pharmaceutical*
558 *and Biomedical Analysis* 168 (2019) 138–147. <https://doi.org/10.1016/j.jpba.2019.02.024>.
- 559 [30] A. Murisier, E. Farsang, K. Horváth, M. Lauber, A. Beck, D. Guillarme, S. Fekete, Tuning
560 selectivity in cation-exchange chromatography applied for monoclonal antibody separations,
561 part 2: Evaluation of recent stationary phases, *J. Pharm. Biomed. Anal.* 172 (2019) 320–328.
562 <https://doi.org/10.1016/j.jpba.2019.05.011>.
- 563 [31] J. Baek, A.B. Schwahn, S. Lin, C.A. Pohl, M. De Pra, S.M. Tremintin, K. Cook, New insights into
564 the chromatography mechanisms of ion-exchange charge variant analysis: Dispelling myths and
565 providing guidance for robust method optimization, *Anal. Chem.* 92 (2020) 13411–13419.
566 <https://doi.org/10.1021/acs.analchem.0c02775>.
- 567 [32] D.V. McCalley, D. Guillarme, Evaluation of additives on reversed-phase chromatography of
568 monoclonal antibodies using a 1000 Å stationary phase, *J. Chromatogr. A* 1610 (2020) 460562.
569 <https://doi.org/10.1016/j.chroma.2019.460562>.
- 570 [33] B. Bobály, A. Beck, J. Fekete, D. Guillarme, S. Fekete, Systematic evaluation of mobile phase
571 additives for the LC–MS characterization of therapeutic proteins, *Talanta* 136 (2015) 60–67.
572 <https://doi.org/10.1016/j.talanta.2014.12.006>.
- 573 [34] M.C. García, The effect of the mobile phase additives on sensitivity in the analysis of peptides
574 and proteins by high-performance liquid chromatography–electrospray mass spectrometry, *J.*
575 *Chromatogr. B* 825 (2005) 111–123. <https://doi.org/10.1016/j.jchromb.2005.03.041>.
- 576 [35] B. Bobály, E. Tóth, L. Drahos, F. Zsila, J. Visy, J. Fekete, K. Vékey, Influence of acid-induced
577 conformational variability on protein separation in reversed phase high performance liquid
578 chromatography, *J. Chromatogr. A* 1325 (2014) 155–162.
579 <https://doi.org/10.1016/j.chroma.2013.12.022>.
- 580 [36] B. Bobály, V. D’Atri, M. Lauber, A. Beck, D. Guillarme, S. Fekete, Characterizing various
581 monoclonal antibodies with milder reversed phase chromatography conditions, *J. Chromatogr.*
582 *B* 1096 (2018) 1–10. <https://doi.org/10.1016/j.jchromb.2018.07.039>.
- 583 [37] V. D’Atri, A. Murisier, S. Fekete, J.-L. Veuthey, D. Guillarme, Current and future trends in
584 reversed-phase liquid chromatography-mass spectrometry of therapeutic proteins, *TrAC -*
585 *Trends Anal. Chem.* 130 (2020) 115962. <https://doi.org/10.1016/j.trac.2020.115962>.
- 586 [38] J.M. Davis, D.R. Stoll, P.W. Carr, Effect of first-dimension undersampling on effective peak
587 capacity in comprehensive two-dimensional separations, *Anal. Chem.* 80 (2008) 461–473.
588 <https://doi.org/10.1021/ac071504j>.
- 589 [39] C. Nowak, J.K. Cheung, S.M. Dellatore, A. Katiyar, R. Bhat, J. Sun, G. Ponniah, A. Neill, B. Mason,
590 A. Beck, H. Liu, Forced degradation of recombinant monoclonal antibodies: A practical guide,
591 *MAbs* 9 (2017) 1217–1230. <https://doi.org/10.1080/19420862.2017.1368602>.
- 592 [40] J. Liigand, R. de Vries, F. Cuyckens, Optimization of flow splitting and make-up flow conditions
593 in liquid chromatography/electrospray ionization mass spectrometry, *Rapid Commun. Mass*
594 *Spectrom.* 33 (2019) 314–322. <https://doi.org/10.1002/rcm.8352>.
- 595 [41] A. Apffel, S. Fischer, G. Goldberg, P.C. Goodley, F.E. Kuhlmann, Enhanced sensitivity for peptide
596 mapping with electrospray liquid chromatography-mass spectrometry in the presence of signal
597 suppression due to trifluoroacetic acid-containing mobile phases, *J. Chromatogr. A* 712 (1995)
598 177–190. [https://doi.org/10.1016/0021-9673\(95\)00175-m](https://doi.org/10.1016/0021-9673(95)00175-m).
- 599 [42] B. Bobály, V. D’Atri, M. Lauber, A. Beck, D. Guillarme, S. Fekete, Characterizing various
600 monoclonal antibodies with milder reversed phase chromatography conditions, *J. Chromatogr.*
601 *B* 1096 (2018) 1–10. <https://doi.org/10.1016/j.jchromb.2018.07.039>.
- 602 [43] S. Chapel, F. Rouvière, S. Heinisch, Pushing the limits of resolving power and analysis time in on-
603 line comprehensive hydrophilic interaction x reversed phase liquid chromatography for the

604 analysis of complex peptide samples, *J. Chromatogr. A* (2019) 460753.
605 <https://doi.org/10.1016/j.chroma.2019.460753>.
606

607 **Figure captions:**

608 **Fig. 1:** 1D-CEX-UV (280 nm) analyses of IdeS-treated ADC-S01 using water + 20 mM MES at pH 6.5 or
609 water + 10 mM phosphate at pH = 6.5 as solvent A using either (a) the Bio MAb NP5 (250 x 2.1 mm, 5
610 μm) column or (b) the BioResolve SCX (100 x 2.1 mm, 3 μm) column . Conditions: solvent A + 300 mM
611 NaCl as solvent B, gradient 1% to 40% B in 20.28 min (BioResolve SCX) or 50.7 min (Bio MAb NP5),
612 flow rate = 0.2 mL/min, temperature = 30°C, injected volume = 5 μL .

613 **Fig. 2:** 1D-RPLC-UV (280 nm) analyses of intact and IdeS-treated ADC-S01 with (a) BioResolve RP
614 mAb polyphenyl (50 x 2.1 mm, 2.7 μm), (b) PLRP-S (50 x 2.1 mm, 5 μm), (c) Biozen intact XB-C8 (50 x
615 2.1 mm, 3.6 μm) and (d) AdvanceBio RP-mAb diphenyl (50 x 2.1 mm, 3.5 μm) columns. Conditions:
616 water + 0.05% TFA + 0.1% FA as solvent A and ACN + 0.05% TFA + 0.1% FA as solvent B, gradient 20%
617 to 95% B in 8.8 min or 7 min (PLRP-S), flow rate = 0.6 mL/min, temperature = 80°C, injected volume =
618 8 μL .

619 **Fig. 3:** (a) 1D-RPLC-UV (280 nm) and (b) 1D-RPLC-HRMS (TIC, ESI+) analyses of IdeS-treated ADC-S01
620 with BioResolve RP mAb polyphenyl (50 x 2.1 mm, 2.7 μm) column. The two dotted horizontal lines
621 delimit the area of interest of the separation. Numbers 1 to 8 indicate the identified species in Table
622 2. Conditions: flow rate = 0.3 mL/min. Same other conditions as in Fig. 2.

623 **Fig. 4:** Contour plot (TIC, ESI+) of the on-line CEX x RPLC analysis of IdeS-treated ADC-S01 used for
624 method development. Conditions in ¹D: flow rate = 0.1 mL/min, gradient 1-40% B in 40.56 min, V_i = 5
625 μL . Conditions in ²D: flow rate = 1.2 mL/min, gradient 20-95% B in 1.1 min, sampling time = 1.5 min
626 (loop volume = 180 μL). Same other conditions as for optimized CEX x RPLC in Table 1. The dotted
627 square indicates the area of interest, the straight line indicates the time below which most of the
628 excipients are eluted in ¹D-CEX and the circle shows the excipients coeluting with the species of
629 interest in ¹D-CEX.

630 **Fig. 5:** Contour plots (TIC, ESI+) of optimized on-line CEX x RPLC analysis of IdeS-treated ADC-S01
631 sample: (a) MS detection (TIC, ESI+) and (b) UV detection (280 nm). See conditions in Table 1.
632 Numbers from 1 to 21 labelled in (a) indicate the species identified in Table 3.

633 **Fig. 6:** Comparison of on-line CEX x RPLC-UV separations of IdeS-treated ADC samples with different
634 levels of stress: (a) non-stressed sample, (b) sample stressed for two weeks, and (c) sample stressed
635 for four weeks. UV detection (280 nm). Conditions are given in Table 1. Numbers from 1 to 22

636 indicate the species identified in Table 3. Main differences between samples highlighted by black
637 dotted circles.

638

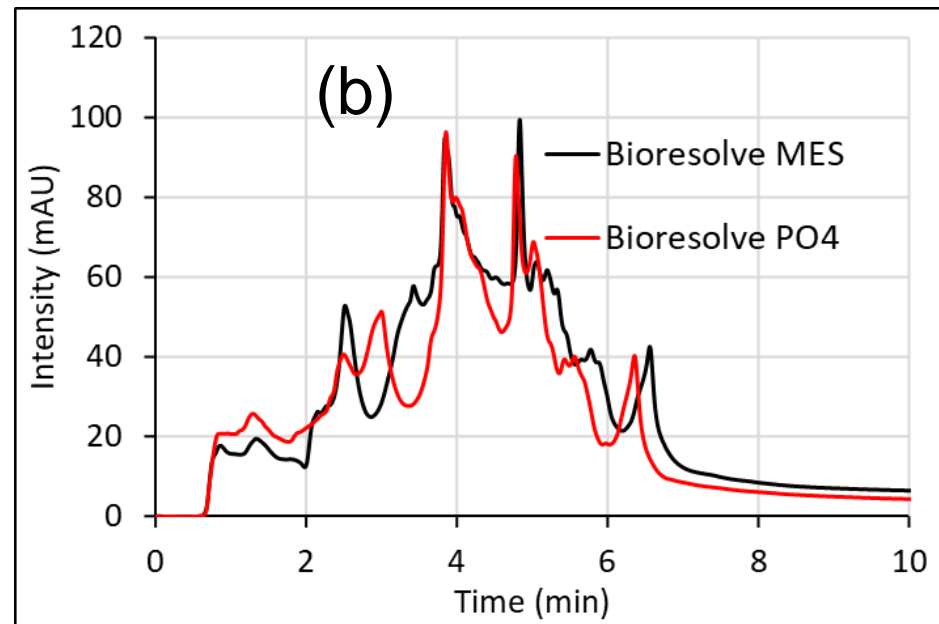
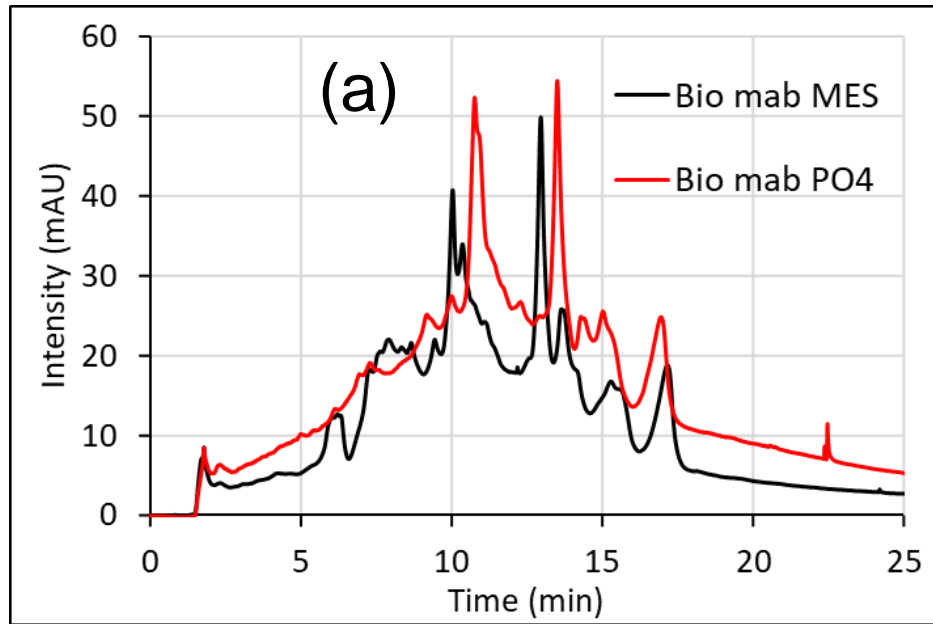
639

640

641

642

643



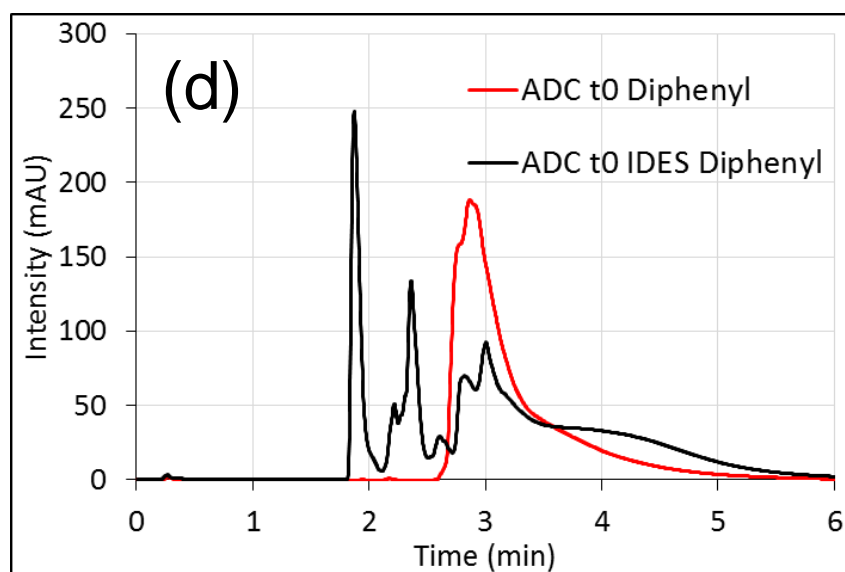
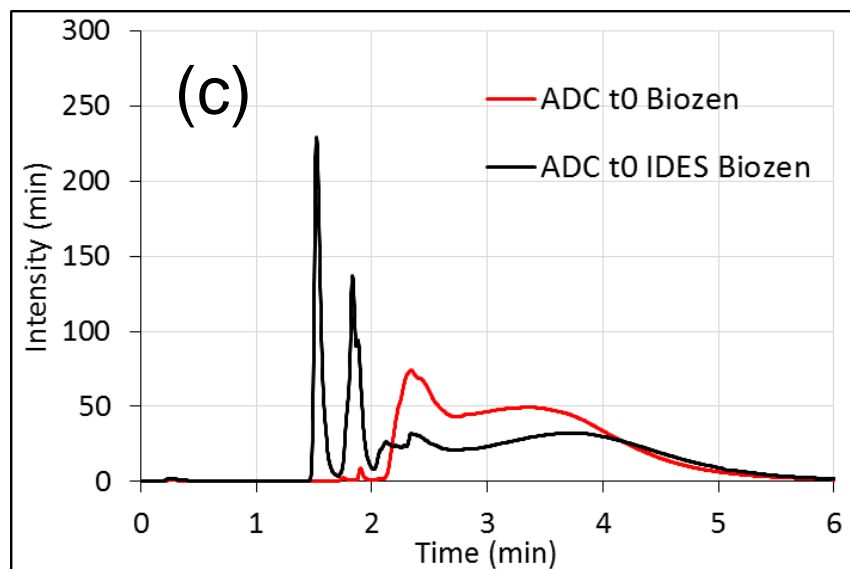
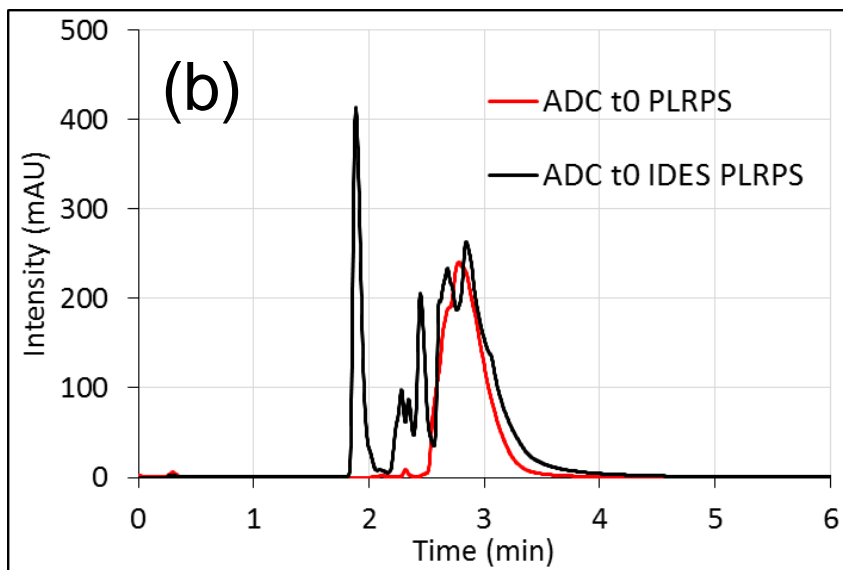
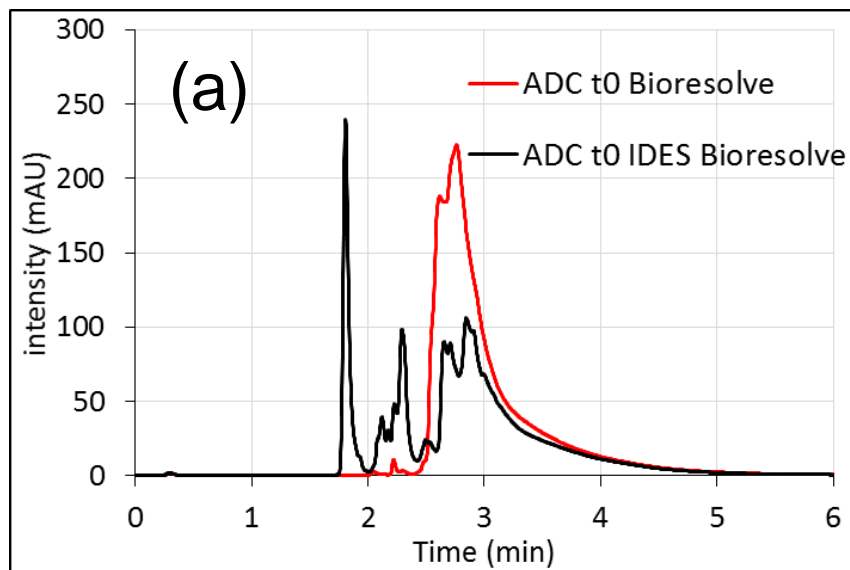


Fig 2

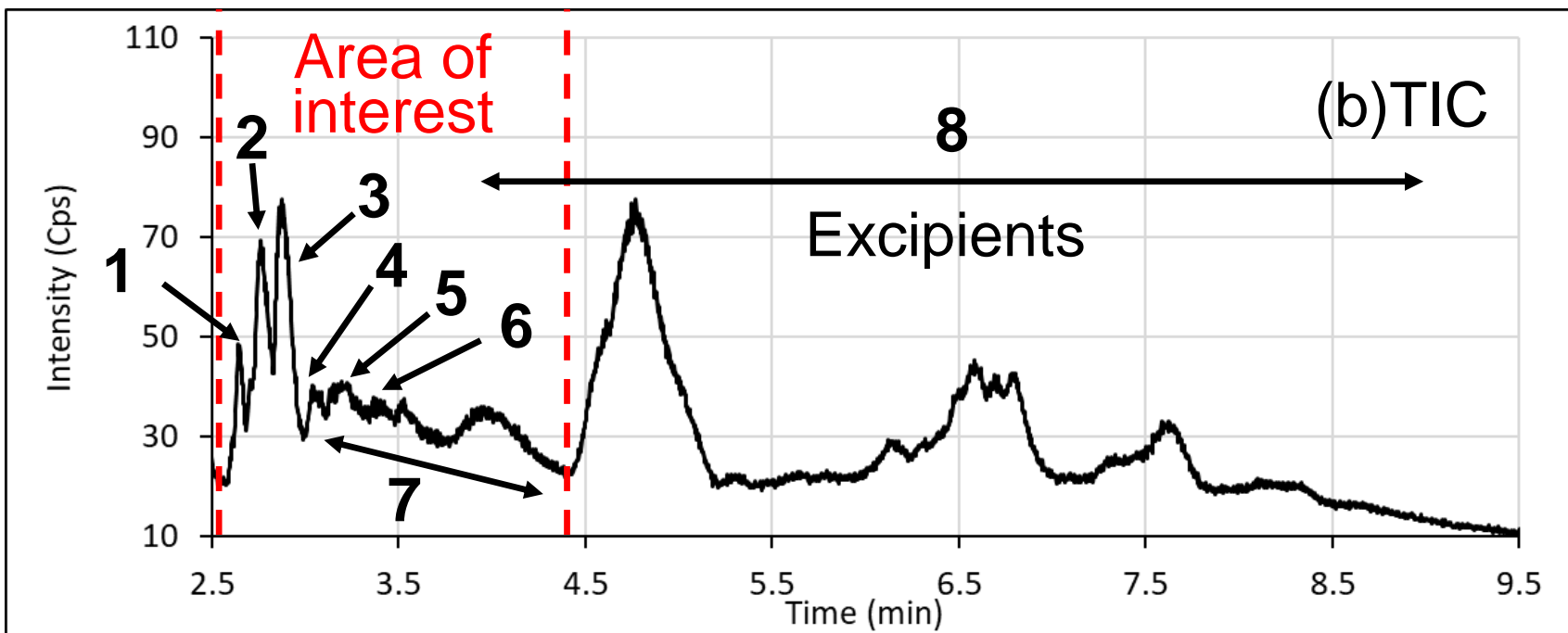
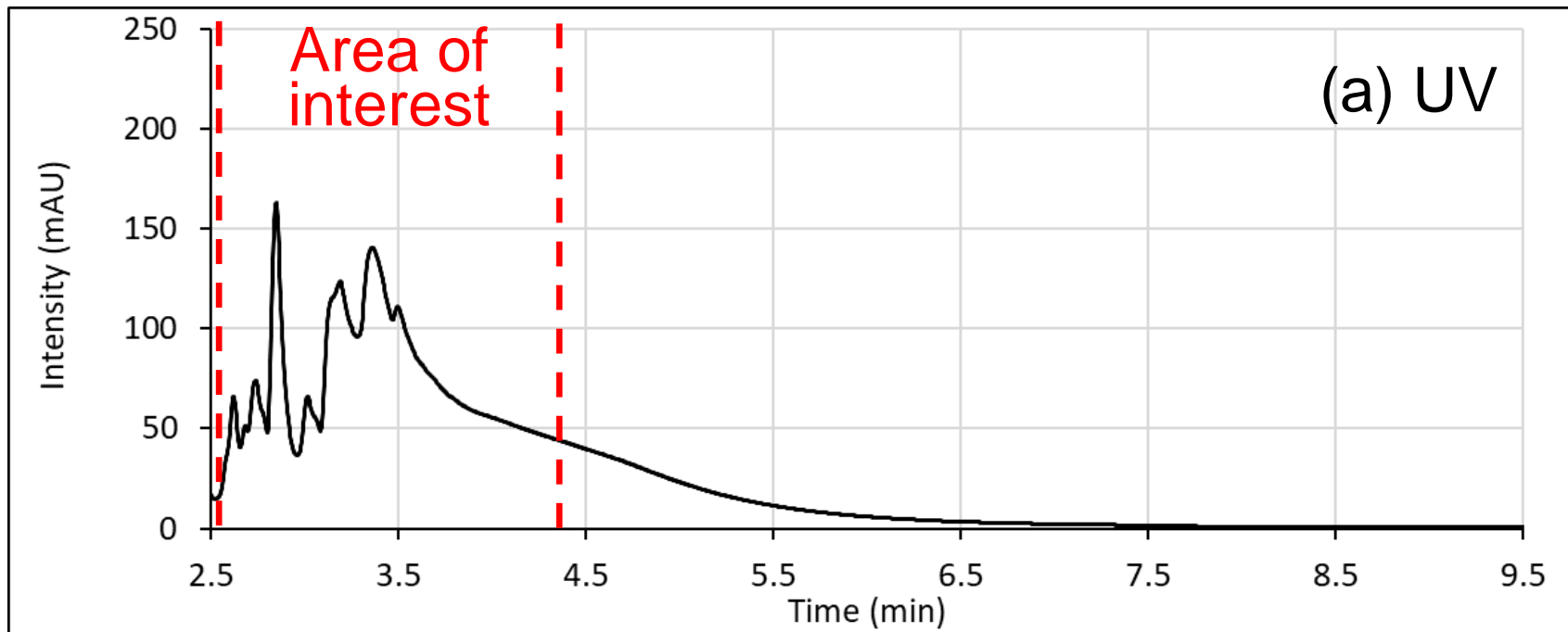


Fig 3

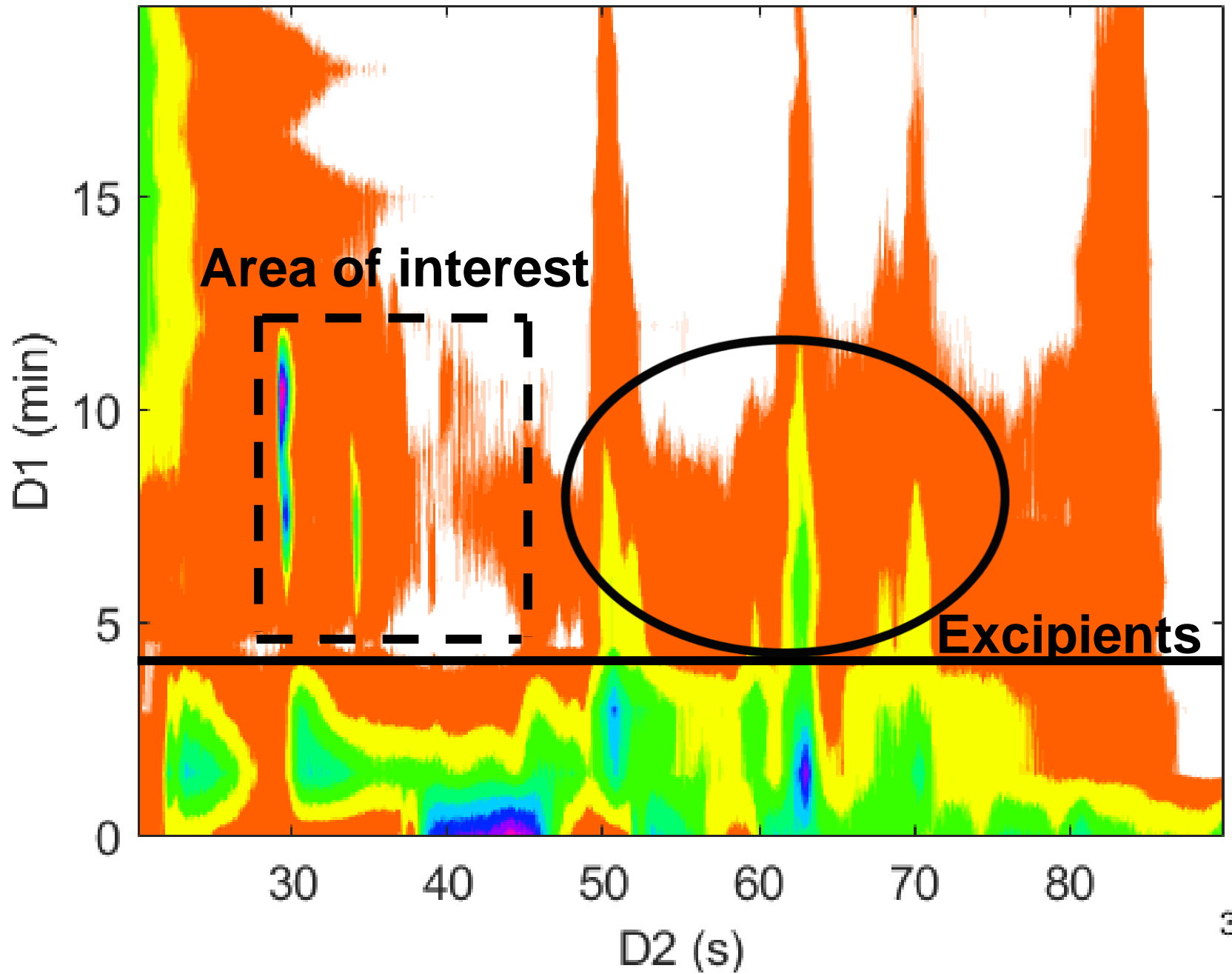


Fig 4

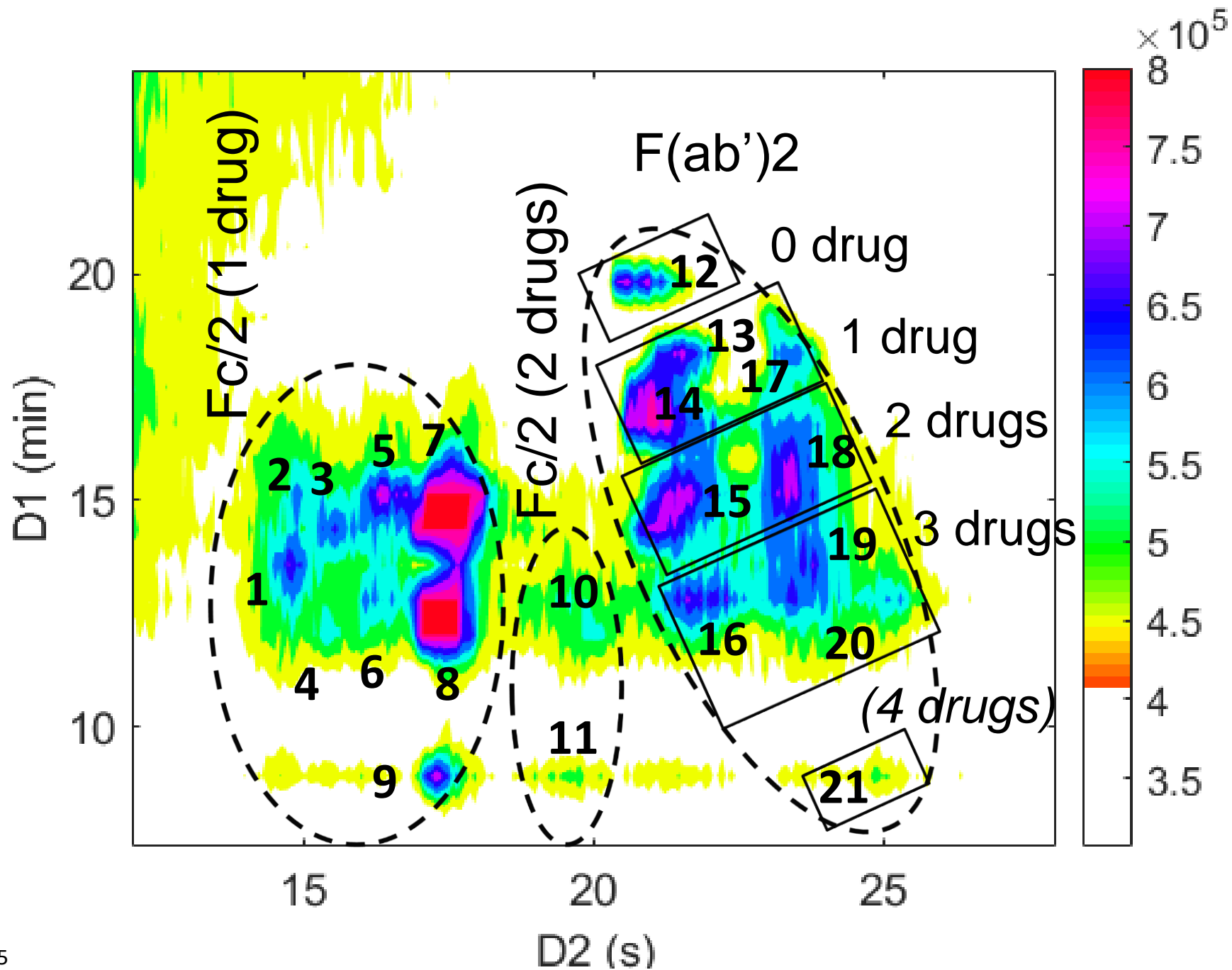


Fig 5

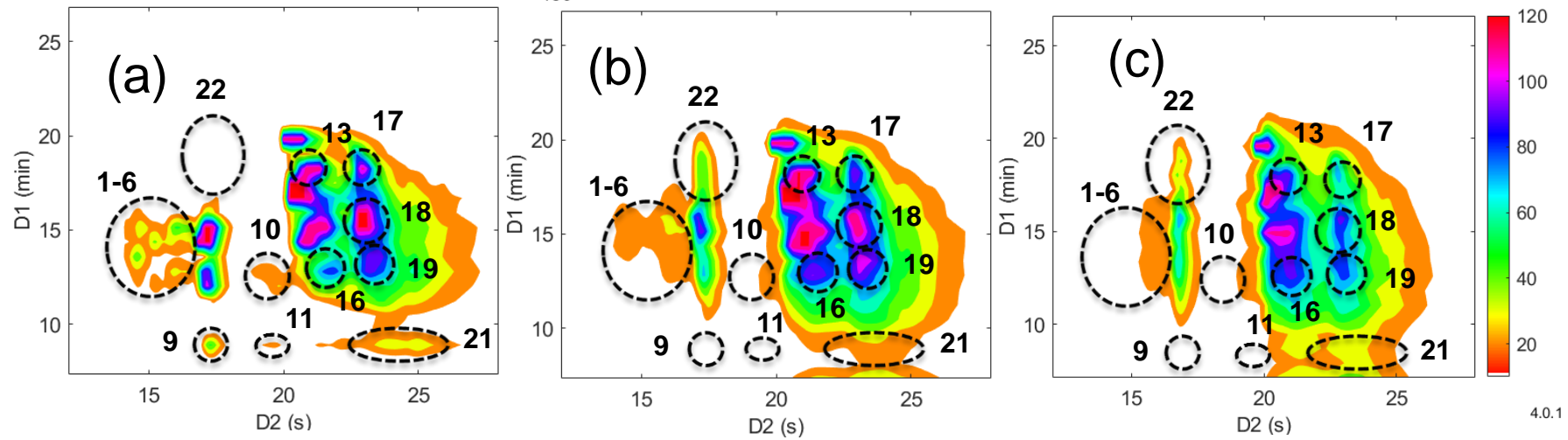


Fig 6

Table 1: Experimental conditions for the optimized CEX x RPLC –UV/HRMS method.

	CEX x RPLC
First dimension (¹D)	
Injection volume	40 µL
Injection solvent	Water
Stationary phase	Bioresolve SCX
Column geometry	(100 x 2.1 mm, 3 µm)
Temperature	30°C
Mobile phase	A: water + 20 mM MES pH = 6.5 B: A + 300 mM NaCl
Flow rate	75 µL/min
Gradient	1-17-1-1% B in 0-20-22.77-31.3 min
Post-column split	/
Modulation	
Loop size	80 µL
Sampling time	0.78 min Starting from 5 min (t ₀ -IdeS and t ₂ -IdeS) or 4 min
Second dimension (²D)	
Stationary phase	Bioresolve RPmAb pk
Column geometry	(50 x 2.1 mm, 2.7 µm)
Temperature	80°C
Mobile phase	A: 0.1% FA + 0.05% TFA in water B: 0.1% FA + 0.05% TFA in ACN
Flow rate	1700 µL/min
Gradient	30-50-30-30% B in 0-0.49-0.55-0.78 min
Post-column split	1:1.5
Diverter valve	Flow to the waste: from 0 to 0.1 min Flow to MS: from 0.1 min to the end
UV detection	280 nm (40 Hz in ¹ D and 80 Hz in ² D)

HRMS detection	
Ionization mode	ESI+
Mass range (Da)	1200-5000
Scan rate (spectra/s)	10
Gas temp (°C)	325
Drying gas (L/min)	13
Nebulizer (psi)	40
Sheath gas (°C)	350
Sheath gas flow (L/min)	12
Capillary voltage (V)	4000
Nozzle voltage (V)	300
Fragmentor (V)	185
Oct 1 Rf Vpp (V)	750
Quad AMU (V)	600

Table 2: Proposed species for the peaks labelled in Fig. 3b after comparison between experimental and theoretical masses.

#	Difference between theoretical and experimental masses (Da)	Proposed specie
1	-1	Fc/2 + 1 drug
2	-1	Fc/2 + 1 drug
3	-1	Fc/2 + 1 drug
4a	-1	Fc/2 + 1 drug
4b	-2	Fc/2 + 2 drugs
5a	+2	(Fab') ₂ + 0 drug
5b	+2	(Fab') ₂ + 1 drug
5c	+2	(Fab') ₂ + 2 drugs
6a	+2	(Fab') ₂ + 1 drug
6b	+1	(Fab') ₂ + 2 drugs
6c	0	(Fab') ₂ + 3 drugs
6d	+1	(Fab') ₂ + 4 drugs
7a	+3	(Fab') ₂ + 0 drug
7b	+2	(Fab') ₂ + 1 drug
7c	+54	(Fab') ₂ + 2 drugs
7d	0	(Fab') ₂ + 3 drugs
7e	-1	(Fab') ₂ + 4 drugs
7f	-1	(Fab') ₂ + 5 drugs

Table 3: Proposed species for the peaks labelled in Figs. 5 and 6.

#	Difference between theoretical and experimental masses (Da)	Proposed specie
1	-3	Fc/2 + 1 drug
2	-3	Fc/2 + 1 drug
3	-3	Fc/2 + 1 drug
4	-1	Fc/2 + 1 drug
5	-3	Fc/2 + 1 drug
6	-2	Fc/2 + 1 drug
7	-3	Fc/2 + 1 drug
8	-3	Fc/2 + 1 drug
9	-3	Fc/2 + 1 drug
10	-4	Fc/2 + 2 drugs
11	-1	Fc/2 + 2 drugs
12	-7	(Fab') ₂ + 0 drug
13	-4	(Fab') ₂ + 1 drug
14	-9	(Fab') ₂ + 1 drug
15	+3	(Fab') ₂ + 2 drugs
16*	+405	(Fab') ₂ + 3 drugs
17*	+198	(Fab') ₂ + 1 drug
18	+11	(Fab') ₂ + 2 drugs
19	+7	(Fab') ₂ + 3 drugs
20	/	/
21	/	/
22	/	/

*:Given the large mass difference between theoretical and experimental deconvoluted masses, these two assignments were made based on the relative positions of the peaks in the contour plot.

Lysine-linked
ADC



Intact ADC
~ 150 kDa

IdeS
→

Partially digested
ADC



F(ab')₂
~ 100 kDa

+



Fc/2 (x 2)
~ 25 kDa

Analysis
→

On-line CEX x RPLC-HRMS
In 30 min

